Supporting Information

Jain et al. 10.1073/pnas.1121319109

SI Materials and Methods

Electronic Structure Model. The electronic structure of the nanorods was described within the real-space screened pseudopotential method (1, 2). We studied a series of nanorods with varying aspect ratios (ξ): $Cd_{256}Se(S)_{255}$ $\xi = 1$, $Cd_{548}Se(S)_{547}$ $\xi = 2$, $Cd_{840}Se(S)_{839}$ $\xi = 3$, $Cd_{1132}Se(S)_{1131}$ $\xi = 4$, $Cd_{1424}Se(S)_{1423}$ $\xi = 5$, $Cd_{1716}Se(S)_{1715}$ $\xi = 6$, $Cd_{2008}Se(S)_{2007}$ $\xi = 7$, $Cd_{2154}Se(S)_{2153}$ $\xi = 7^{1/2}$, and $Cd_{2300}Se(S)_{2299}$ $\xi = 8$. In Fig. 1, we showed the structure of CdSe and CdS nanorods with an aspect ratio $\xi = 8$.

To obtain the lowest transitions and calculate the absorption cross-section, we used the filter diagonalization approach (3). The quasiparticle gaps calculated for the nanorods are summarized in Table S1. Within the accuracy of the calculation, we found that above $\xi = 4$ the quasiparticle gap is independent of the length of the nanorod (L).

Near-Field Absorption. The average rate of energy absorption of an electronic system subject to a time-dependent external homogeneous electric field $E_z(t)$ is given by:

$$P = \frac{1}{2T}\int_{-T}^{T} \dot{E}_z(t) D_z(t) dt, \qquad \text{[S1]}$$

where T is an average time and D_z is the expectation value of the electronic dipole, determined by

$$D_z(t) = -e\int n_1(r,t) z d^3r, \qquad \text{[S2]}$$

$n_1(r,t) = n(r,t) - n_0(r)$ is the response density, $n(r,t)$ is the electron density as driven by the field, and $n_0(r)$ is the ground state density. The density is linearly related to the perturbing potential via the response function χ_{nn}

$$n_1(r,t) = \int_0^\infty d\tau \int \chi_{nn}(r,r',\tau) e v_{ext}(r',t-\tau) d^3r', \qquad \text{[S3]}$$

where, $v_{ext}(r,t) = E_z(t) z$ is the potential of the external electromagnetic field, and $\chi_{nn}(r,r',\tau)$ is the density-density response function:

$$\chi_{nn}(r,r',t) = -\frac{i}{\hbar}\theta(t)\langle\Psi_0|[\hat{n}(r,t),\hat{n}(r')]|\Psi_0\rangle. \qquad \text{[S4]}$$

In addition, $\hbar$ is Planck's constant divided by 2π. In the above, Ψ_0 is the many body ground state of the electrons. When the perturbing field is sinusoidal of frequency ω, $E_z(t) = E_0 e^{i\omega t} + c$ it is natural to work in frequency domain. In this case, the rate of photon absorption is the rate of energy absorption by $\hbar\omega$:

$$\Gamma(\omega) = \frac{P}{\hbar\omega} = -\frac{2}{\hbar} lm[eE_0 \int n_1(r,\omega) z d^3r]. \qquad \text{[S5]}$$

In this expression, the Fourier transformed density is:

$$n_1(r,\omega) \equiv \lim_{T\to\infty}\frac{1}{2T}\int_{-T}^{T} e^{i\omega t} n_1(r,t) dt. \qquad \text{[S6]}$$

In frequency domain, the analog of Eq. **S3** is

$$n_1(r,\omega) = \int \chi_{nn}(r,r',\omega) e v_{ext}(r',\omega) d^3r'. \qquad \text{[S7]}$$

Where, the potential in frequency domain is

$$v_{ext}(r,\omega') = \frac{1}{2T}\int_{-T}^{T} e^{-i\omega' t} E_0 z e^{i\omega t} dt = E_0 z\left[\frac{\sin(\omega-\omega')T}{(\omega-\omega')T}\right] \to z E_0 \delta_{\omega,\omega'}. \qquad \text{[S8]}$$

In addition, the Fourier transformed density-density response is

$$\chi_{nn}(r,r',\omega) = \int_0^\infty e^{i\omega\tau}\chi_{nn}(r,r',\tau) d\tau. \qquad \text{[S9]}$$

One can use the Lehman representation for χ,

$$\chi_{nn}(r,r',\omega) = \sum_{I>0}\left[\frac{n_{0I}(r) n_{I0}(r')}{\hbar\omega - (\mathscr{E}_I - \mathscr{E}_0) + i\eta} - \frac{n_{0I}(r) n_{I0}(r')}{\hbar\omega + (\mathscr{E}_I - \mathscr{E}_0) + i\eta}\right], \qquad \text{[S10]}$$

where, $n_{0I}(r) = \langle\Psi_0|\hat{n}(r)|\Psi_I\rangle$ and $\mathscr{E}_1$, Ψ_I are the many-electron eigenenergies and eigenstates. For $\omega > 0$

$$Im[\chi_{nn}(r,r',\omega)] = -\pi\sum_{I>0} n_{0I}(r) n_{I0}(r')\delta[\hbar\omega - (\mathscr{E}_1 - \mathscr{E}_0)]. \qquad \text{[S11]}$$

We will use a shorthand notation for Eq. **S7**,

$$n_1 = \chi e v_{ext}. \qquad \text{[S12]}$$

Note that in this equation, χ was viewed as an integral operator transforming a potential energy $e v_{ext}(r')$ to a Fourier-transformed density $n_1(r,\omega)$.

Using the shorthand notation, the absorption spectrum is

$$\Gamma(\omega) = -\frac{2}{\hbar}|eE_0|^2 Im[z\chi_{nn}z], \qquad \text{[S13]}$$

where now $z\chi z$ is a double integral.

$$z\chi_{nn}z \equiv \iint z\chi(r,r',\omega) z' d^3r' d^3r. \qquad \text{[S14]}$$

Now, suppose that the system is composed of two spatially distinct parts: A and B. The interaction between the systems is weak, and we treated it perturbatively. We assume that both systems were neutral and has no dipole moment in the ground state, so that, neglecting van der Waals interaction, they interact only in the excited states. In our perturbative approach the response density of each part to an external potential v_{ext} is written, as follows:

$$n_1^A = \chi_{nn}^{AA} e v_{ext} + \chi_{nn}^{AB} e v_{ext} \qquad n_1^B = \chi_{nn}^{BB} e v_{ext} + \chi_{nn}^{BA} e v_{ext}, \qquad \text{[S15]}$$

where, χ_{nn}^{AA} and χ_{nn}^{BB} are the unperturbed density-density response functions of systems A and B, respectively. These

responses were corrected by the interaction between the systems and were denoted as χ_{nn}^{AB} and χ_{nn}^{BA}. The intersystem effect is due to the long-range electron-electron interaction. We neglect exchange-correlation effects between the two systems; thus, only time-dependent Hartree interaction is included. This Hartree interaction creates a potential in A due to the density perturbation in B:

$$v_H^{AB}(r_A,\omega) = \frac{e}{4\pi\epsilon_0}\int \frac{n_1^B(r_B,\omega)}{|r_A - r_B|} d^3 r_B. \qquad \textbf{[S16]}$$

Alternatively, in compact notation, we use this equation to define an integral operator C^{AB}, as follows:

$$ev_H^{AB} = C^{AB} n_1^B. \qquad \textbf{[S17]}$$

Note that the integral is done over the volume of B, and that it has results in the volume of A. We also define an operator C^{BA} in an analogous manner with the roles of A and B interchanged. The potential v_H^{AB} in A now creates an additional charge distortion in A given by $\chi_{nn}^{AA} e v_H^{AB}$. Thus, the interaction between the systems is

$$\chi_{nn}^{AB} e v_{ext} = \chi_{nn}^{AA} e v_H^{AB} \qquad \chi_{nn}^{BA} e v_{ext} = \chi_{nn}^{BB} e v_H^{BA}.$$

The following relations in our perturbative approach can then be derived as

$$n_1^A = \chi_{nn}^{AA} e v_{ext} + \chi_{nn}^{AA} C^{AB} n_1^B \qquad n_1^B = \chi_{nn}^{BB} e v_{ext} + \chi_{nn}^{BB} C^{BA} n_1^A. \qquad \textbf{[S18]}$$

Combining these equations and solving for the density perturbations, we obtain an exact adiabatic result for the system

$$\begin{aligned} n_1^A &= (1^{AA} - \chi_{nn}^{AA} C^{AB} \chi_{nn}^{BB} C^{BA})^{-1} \chi_{nn}^{AA} (1^{AA} + C^{AB} \chi_{nn}^{BB}) e v_{ext} \\ n_1^B &= (1^{BB} - \chi_{nn}^{BB} C^{BA} \chi_{nn}^{AA} C^{AB})^{-1} \chi_{nn}^{BB} (1^{BB} + C^{BA} \chi_{nn}^{AA}) e v_{ext}, \end{aligned} \qquad \textbf{[S19]}$$

where $1^{AA} = \delta(r_A - r_A')$. This relation takes account of the effect of A on B and B on A. One can then rewrite the result for χ_{nn} based on Eq. **S10** in terms of the separate χ_{nn}^A and χ_{nn}^B

$$\begin{aligned} \chi_{nn} = &(1^{AA} - \chi_{nn}^{AA} C^{AB} \chi_{nn}^{BB} C^{BA})^{-1} \chi_{nn}^{AA} (1^{AA} + C^{AB} \chi_{nn}^{BB}) \\ &+ (1^{BB} - \chi_{nn}^{BB} C^{BA} \chi_{nn}^{AA} C^{AB})^{-1} \chi_{nn}^{BB} (1^{BB} + C^{BA} \chi_{nn}^{AA}). \end{aligned} \qquad \textbf{[S20]}$$

Up to now we did not make an approximation concerning the strength of the Hartree interaction between A and B. We now assume a small interaction and expand to second order in C, obtaining

$$\begin{aligned} \chi_{nn} = &\chi_{nn}^{AA} + \chi_{nn}^{BB} + 2\chi_{nn}^{BB} C^{BA} \chi_{nn}^{AA} + \chi_{nn}^{BB} C^{BA} \chi_{nn}^{AA} C^{AB} \chi_{nn}^{BB} \\ &+ \chi_{nn}^{AA} C^{AB} \chi_{nn}^{BB} C^{BA} \chi_{nn}^{AA}. \end{aligned} \qquad \textbf{[S21]}$$

Furthermore, if we assume that A was the sphere with much larger polarizability than the rod, we can neglect the term $\chi_{nn}^{BB} C^{BA} \chi_{nn}^{AA} C^{AB} \chi_{nn}^{BB}$ and have

$$\begin{aligned} z\chi_{nn} z &= z\chi_{nn}^{AA} z + z\chi_{nn}^{BB} z + 2z\chi_{nn}^{BB}\zeta + \zeta\chi_{nn}^{BB}\zeta \\ &= z\chi_{nn}^{AA} z + (z+\zeta)\chi_{nn}^{BB}(z+\zeta). \end{aligned} \qquad \textbf{[S22]}$$

Where, by $\zeta = C^{BA}\chi_{nn}^{AA} z$ we have

$$\zeta(r,\omega) = \iint \frac{e^2}{4\pi\epsilon_0 |r - r'|} \chi_{nn}^{AA}(r', r'', \omega) z'' d^3 r'' d^3 r'$$

and $v_H(r,\omega) = E_0\zeta(r,\omega)$ is the Hartree potential in B due to a *dipole* potential perturbation $E_0 z$ in A. Inserting this expression into Eq. **S11** leads to the following absorption rate:

$$\Gamma(\omega) = \Gamma_A(\omega) - \frac{2}{\hbar}|eE_0|^2 Im\{[z + \zeta(\omega)]\chi_{nn}^{BB}(\omega)[z + \zeta(\omega)]\}. \qquad \textbf{[S23]}$$

Or, using Eq. **S9**:

$$\Gamma(\omega) = \Gamma_A(\omega) + \frac{2\pi}{\hbar}\sum_{I>0} |eE_0[z_{I0}^B + \zeta_{I0}^B(\omega)]|^2 \delta[\hbar\omega - (\mathscr{E}_1^B - \mathscr{E}_0^B)], \qquad \textbf{[S24]}$$

where $z_{I0}^B = \langle \Psi_I^B | \sum_n \hat{z}_n | \Psi_0^B \rangle$ and $\zeta_{I0}^B(\omega) = \langle \Psi_1^B | \sum_n \zeta(\hat{r}_n, \omega) | \Psi_0^B \rangle$, Ψ_I^B is the Ith many-electron eigenstate of system B, and n sums over all electrons in B. For noninteracting electrons, these transition moments are nonzero only for single electron excitations from the ground state determinantal wave function, and the sum over excited states can be written as a sum over electron-hole pairs, as follows:

$$\Gamma(\omega) = \Gamma_A(\omega) + \frac{2\pi}{\hbar}\sum_{aj} |\langle \psi_a | e\hat{\phi}(\omega) | \psi_j \rangle|^2 \delta[\hbar\omega - (\varepsilon_a - \varepsilon_j)], \qquad \textbf{[S25]}$$

where

$$\ddot{\phi} \equiv \phi(\hat{r}) = -E_0^*[\hat{z} + \zeta(\hat{r},\omega)]. \qquad \textbf{[S26]}$$

Eq. **S22** is the expression used in the manuscript.

Near-Field Calculations. To obtain the near-field generated by the metal tip, we followed standard procedures based on solving the relevant Maxwell equations

$$\nabla \cdot D(r,\omega) = \rho(r,\omega), \qquad \textbf{[S27]}$$

where $\rho(r,\omega)$ was the spatial electric density at frequency ω and $D(r,\omega) = \epsilon(r,\omega)E(r,\omega)$ was the electric displacement related linearly to the electric field $E(r,\omega)$ through the dielectric medium with constant $\epsilon(r,\omega)$. In typical cases, the transverse component of the electric field is negligible, so $E(r,\omega) \approx -\nabla\phi(r,\omega)$, where $\phi(r,\omega)$ was the electric potential, thus

$$-\nabla \cdot [\epsilon(r,\omega)\nabla\phi(r,\omega)] = \rho(r,\omega). \qquad \textbf{[S28]}$$

When the external field $E_0(\omega)$ is homogeneous the potential is given by $\phi(r,\omega) = -E_0(\omega)\cdot r + \varphi(r,\omega)$, where $\varphi(r,\omega) \to 0$ as $r \to \infty$

$$-\nabla \cdot [\epsilon(r,\omega)\nabla\varphi(r,\omega)] = \rho(r,\omega). \qquad \textbf{[S29]}$$

For a sphere of radius a and dielectric constant $\epsilon_1(\omega)$ embedded in an infinite medium of dielectric constant $\epsilon_m(\omega)$ and an external field $E_0(\omega)$ in the z direction, this equation has a simple solution outside the sphere

$$\phi_+(r,\omega) = -E_0(\omega) z\left[1 - s(\omega)\left(\frac{a}{r}\right)^3\right], \qquad \textbf{[S30]}$$

and, inside the sphere

$$\phi_{-}(r,\omega) = -E_0(\omega)z[1-s(\omega)], \qquad \text{[S31]}$$

with

$$s(\omega) = \frac{\epsilon_1(\omega)-\epsilon_m(\omega)}{\epsilon_1(\omega)+2\epsilon_m(\omega)}. \qquad \text{[S32]}$$

In Fig. S2, we plotted $\epsilon_1(\omega)$ and for $s(\omega)$ gold and silver, assuming the surrounding medium had a refractive index of 1.45.

Comparing Eq. **S29** to Eq. **S26** we saw that in the present case, the induced potential in the rod resulting from the sphere was $E_0\zeta(r,\omega) = -E_0 z s(\omega)(\frac{a}{r})^3$.

Selection Rules Based on an Effective Mass Model for a Cylinder. Whereas the single band effective mass model is a crude approximation to the electronic structure of the nanorod, it provides means to analyze the results based on the atomistic calculations in simple terms. Within the single band effective mass model, one assumes that the electron (hole) wave functions were given by a product of and envelop function and a Bloch function

$$\psi_e(r) = \varphi_e(r)u_c(r) \qquad \psi_h(r) = \varphi_h(r)u_v(r), \qquad \text{[S33]}$$

where $\varphi_{e,h}(r)$ is the envelop function and $u_{c,v}(r)$ is the Bloch function for the valance (v) and conduction (c) bands. The matrix element determining the selection rules is given by

$$\begin{aligned} A &= \langle\psi_e|e\hat{\phi}(\omega)|\psi_h\rangle \\ &= e\Omega_{\text{cell}}\sum_L\int_0 \varphi_h(r+L)u_v(r)\phi(r+L,\omega)u_c(r)\varphi_e(r+L)d^3r \\ &= e\Omega_{\text{cell}}\sum_L\varphi_h(L)\varphi_e(L)\int_0 u_v(r)\phi(r+L)u_c(r)d^3r. \end{aligned} \qquad \text{[S34]}$$

Where, e is the electron charge, $\phi(r,\omega) = -E_0(\omega)z[1-s(\omega)(\frac{a}{r})^3] \equiv -E_0(\omega)z + \delta\phi(r,\omega)$, the sum is over all unit cells, and the remaining integral is over a unit cell. Using the conventional assumptions of the effective mass model and defining $\delta A = \langle\psi_e|e\hat{\phi}(\omega)|\psi_h\rangle + \langle\psi_e|eE_0(\omega)z|\psi_h\rangle$, we found

$$\begin{aligned} \delta A &= \text{es}(\omega)E_0(\omega)a^3\Omega_{\text{cell}}\sum_L\varphi_h(L)\varphi_e(L)\frac{1}{|L+a\hat{z}|^3} \\ &\quad\times\int_0 u_v(r)(z+L_z)\left[1-3r\cdot\frac{(L+a\hat{z})}{|L+a\hat{z}|^2}\right]u_c(r)d^3r, \end{aligned} \qquad \text{[S35]}$$

where we used the approximation

$$\frac{(z+L_z)}{|r+L+a\hat{z}|^3} \approx \frac{(z+L_z)}{|L+a\hat{z}|^3} - 3r\cdot(L+a\hat{z})\frac{(z+L_z)}{|L+a\hat{z}|^5}. \qquad \text{[S36]}$$

The integration over the unit cell was simplified to yield:

$$\begin{aligned} & e\int_0 u_v(r)(z+L_z)\left[1-3r\cdot\frac{(L-a\hat{z})}{|L-a\hat{z}|^2}\right]u_c(r)d^3r \\ &\approx e\int_0 u_v(r)zu_c(r)d^3r - \frac{3eL_z}{|L+a\hat{z}|^2}\int_0 u_v(r)[r\cdot(L-a\hat{z})]u_c(r)d^3r \\ &= d_b - \frac{3L_z[d_b\cdot(L+\hat{z}a)]}{|L+a\hat{z}|^2}. \end{aligned} \qquad \text{[S37]}$$

Inserting this expression into the expression for δA, we found

$$\begin{aligned} \delta A &= s(\omega)E_0(\omega)a^3\Omega_{\text{cell}}\sum_L\varphi_h(L)\varphi_e(L)\frac{1}{|L+a\hat{z}|^3} \\ &\quad\times\left\{d_b - \frac{3L_z[d_b\cdot(L+a\hat{z})]}{|L+a\hat{z}|^2}\right\} \\ &= \text{es}(\omega)E_0(\omega)a^3\int d^3r\varphi_h(r)\varphi_e(r)\frac{1}{|r+a\hat{z}|^3} \\ &\quad\times\left\{d_b - \frac{3z[d_b\cdot(r+a\hat{z})]}{|r+a\hat{z}|^2}\right\} \end{aligned} \qquad \text{[S38]}$$

and

$$\begin{aligned} A &= A_{\text{dip}} + s(\omega)E_0(\omega)a^3\Omega_{\text{cell}}\sum_L\varphi_h(L)\varphi_e(L)\frac{1}{|L+a\hat{z}|^3} \\ &\quad\times\left\{d_b - \frac{3L_z[d_b\cdot(L+a\hat{z})]}{|L+a\hat{z}|^2}\right\} \\ &= A_{\text{dip}} + \text{es}(\omega)E_0(\omega)a^3\int d^3r\varphi_h(r)\varphi_e(r)\frac{1}{|r+a\hat{z}|^3} \\ &\quad\times\left\{d_b - \frac{3z[d_b\cdot(r+a\hat{z})]}{|L+a\hat{z}|^2}\right\}, \end{aligned} \qquad \text{[S39]}$$

where (4)

$$A_{\text{dip}} = d_b\int d^3r\varphi_h(r)\varphi_e(r). \qquad \text{[S40]}$$

The dipolar term (A_{dip}) leads to strict selection rules where the quantum numbers of the electron and hole were preserved upon excitation resulting from the above overlap integral. That is no longer the case in the presence of a near-field, where the leading term

$$s(\omega)E_0(\omega)a^3d_b\int d^3r\varphi_h(r)\varphi_e(r)\frac{1}{|r+a\hat{z}|^3}$$

does not vanish even when the electron and hole quantum numbers in the longitudinal direction differ.

Convergence Tests. A typical spectrum of a CdSe nanorod with aspect ratio of $\xi = 7^{1/2}$ is shown in Fig. S3 for a near-field generated from a gold nanoparticle of diameter $D = 10$ nm. The calculation show that the first peak in the absorption spectrum is converged with approximately 300 filtered states.

Dielectric Function for CdSe Nanocrystals. The dielectric function for the semiconductor was generated from the real-space pseudopotential model taking into account quantum confinement effects. The complex dielectric function is given by

$$\epsilon(\omega) = 1 - \frac{4\pi}{V}\frac{e^2\hbar^2}{m_e 4\pi\epsilon_0}\sum_{ja}\frac{f_{aj}}{(\hbar\omega)^2 - \varepsilon_{aj}^2 + 2iE\Gamma_{pp}}, \qquad \text{[S41]}$$

where V is the volume of the nanoparticle, m_e and e are the electron's mass and charge, respectively, and ϵ_0 is the vacuum permittivity. In the results shown below, $\Gamma_{pp} = 0.1$ eV is the broadening parameter, $\varepsilon_{aj} = \varepsilon_a - \varepsilon_j$ is the energy difference between an electron in state a (conduction electron) and an electron in state j (valance electron), and f_{aj} is the oscillator strength given by

$$f_{aj} = 2\frac{2m_e\varepsilon_{aj}}{3\hbar^2 e^2}\left(|\langle\phi_a|u_x|\phi_j\rangle|^2 + |\langle\phi_a|\mu_y|\phi_j\rangle|^2 + |\langle\phi_a|\mu_z|\phi_j\rangle|^2\right), \quad \textbf{[S42]}$$

where, as before, $\mu_{x,y,z}$ was the dipole operator, $\langle r|\phi_a\rangle$ and $\langle r|\phi_j\rangle$ were the conduction and valance single particle wave functions, respectively, which were the solution of real-space pseudopotential model.

For convergence purposes, we subtracted the zero frequency dielectric const function from the above equation and added the experimental value $\epsilon(0)$:

$$\epsilon(\hbar\omega) = \epsilon(0) - \frac{4\pi}{V}\frac{e^2\hbar^2}{m_e 4\pi\epsilon_0}\sum_{ja} f_{aj}\left[\frac{1}{(\hbar\omega)^2 - \varepsilon_{aj}^2 + 2iE\Gamma_{pp}} + \frac{1}{\varepsilon_{aj}^2}\right]. \quad \textbf{[S43]}$$

The results for CdSe nanocrystals of varying diameters are shown in Fig. S4. These are in good agreement with other calculations for CdSe nanocrystals (5) and seem to converge to the results known for bulk CdSe (6).

Band Bending. An alternative source that may lead to the observed spectral shifts was due to band bending. To equilibrate the chemical potentials of the metal and semiconductors, charges would move from the semiconductor to the metal if its Fermi energy was above that of the metal and vice versa. The migration of charges led to a field across the interface that caused the bands of the semiconductor to bend (7). This bending could also lead to spectral shifts.

In Fig. 5, we plotted the absorption spectrum of a CdSe nanorod for two aspect ratio $\xi = 4$ and $\xi = 8$. Two limiting cases of bending were shown, positive and negative. Bending is modeled by adding a constant energy (± 2 eV) to the ligand potentials on one size of the nanorod. This procedure leads to an addition field at the nanorod's edge of ≈ 5 V/nm used to represent the field generated at the metal-semiconductors junction. As could be seen, band bending led to a red shift in the optical spectrum in contrast to the blue shift observed experimentally. Moreover, the shift was quite small, approximately 1 nm for the fields described above.

If bending was a source of spectral shifts, and if it would lead to blue shifts (which it does not), then one would expect the magnitude of the shift to saturate when the Fermi energy of the metal nanoparticle approaches the bulk value. This effect typically occurs at nanoparticle size below 200 atoms; however, the fact that the spectral shift continued to grow with the plasmon intensity was another indication that band bending was not a significant source of spectral shifts.

1. Rabani E, Hetenyi B, Berne BJ, Brus LE (1999) Electronic properties of CdSe nanocrystals in the absence and presence of a dielectric medium. *J Chem Phys* 110:5355–5369.
2. Toledo S, Rabani E. (2002) Very large electronic structure calculations using an out-of-core filter-diagonalization method. *J Comp Physiol* 180:256–269.
3. Wall MR, Neuhauser D (1995) Extraction, through filter-diagonalization, of general quantum eigenvalues or classical normal-mode frequencies from a small number of residues or a short-time segment of a signal. 1. Theory and application to a quantum-dynamics model. *J Chem Phys* 102:8011–8022.
4. Haug H, Koch SW (2004) *Quantum Theory of the Optical and Electronic Properties of Semiconductors* (World Scientific, Singapore; River Edge, NJ).
5. Alves-Santos M, Di Felice R, Goldoni G (2010) Dielectric functions of semiconductor nanoparticles from the optical absorption spectrum: The case of CdSe and CdS, *J Phys Chem C* 114:3776–3780.
6. Kim YD (1994) Optical-properties of zinc-blende Cdse and Zn(X)Cd(1-X)Se films grown on GaAs. *Phys Rev B* 49:7262–7270.
7. Nozik AJ, Memming R (1996) Physical chemistry of semiconductor-liquid interfaces. *J Phys Chem* 100:13061–13078.

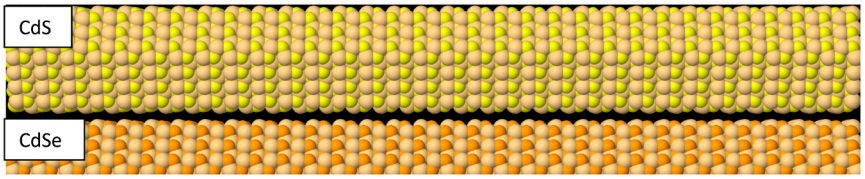

Fig. S1. Images of CdS (*Upper*) and CdSe (*Lower*) nanorods used in the atomistic calculations with an aspect ratio of $\xi = 8$.

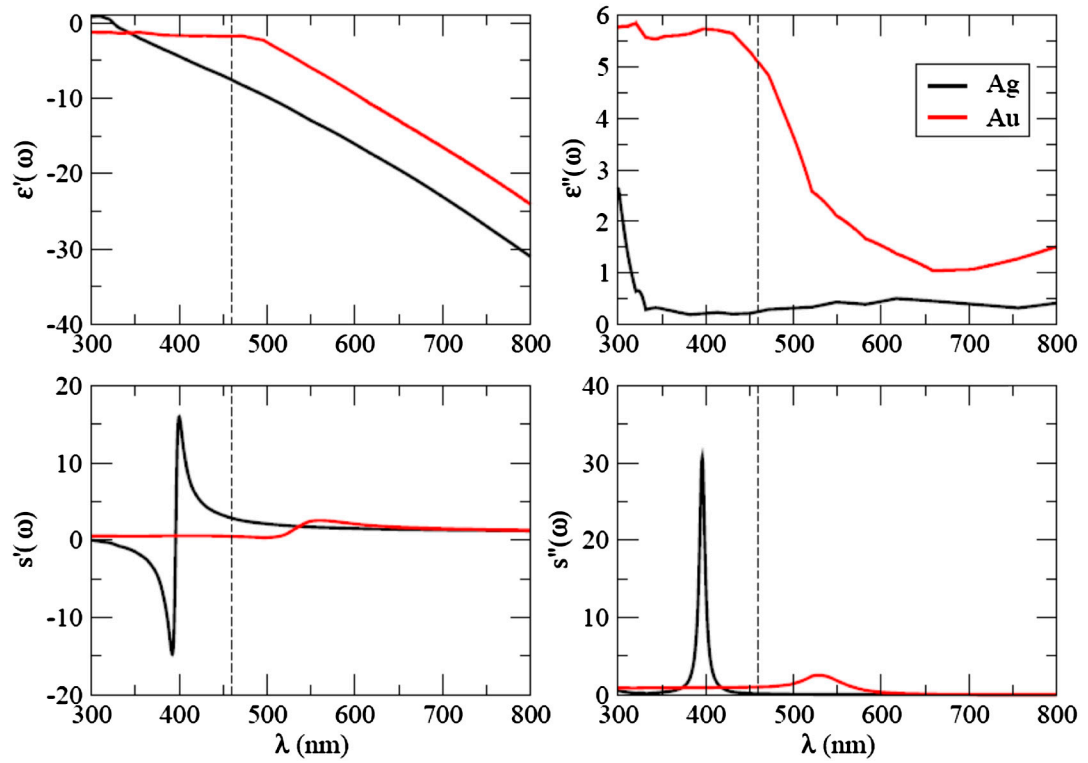

Fig. S2. Real and imaginary parts of the dielectric constant $\epsilon_1(\omega) = \epsilon_1'(\omega) + i\epsilon_1''(\omega)$ and $s(\omega) = s'(\omega) + is''(\omega)$ for silver (black curves) and gold (red curves).

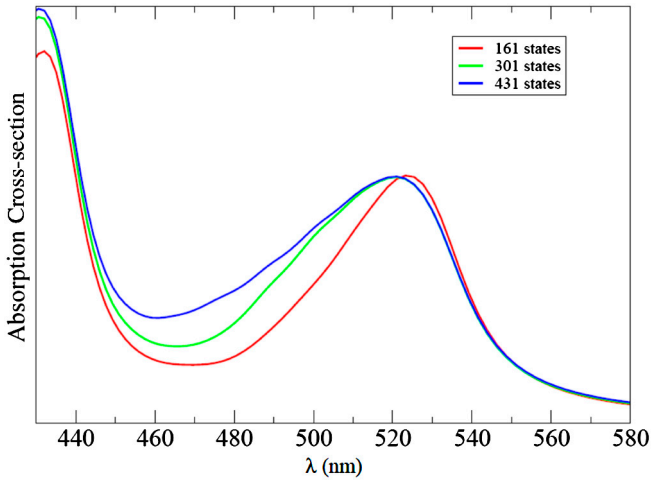

Fig. S3. Absorption cross-section of a CdSe nanorod with an aspect ratio of $\xi = 7^{1/2}$ for different number of filtered states near the band edge.

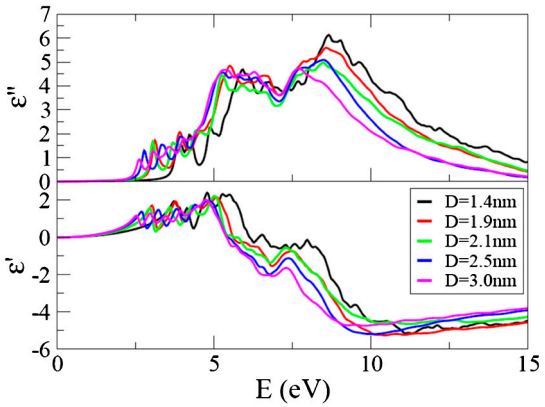

Fig. S4. Real and imaginary part of the dielectric function calculated from the real-space pseudopotential model for CdSe nanocrystals of varying diameters. The value of $\epsilon(0)$ is subtracted from the real part.

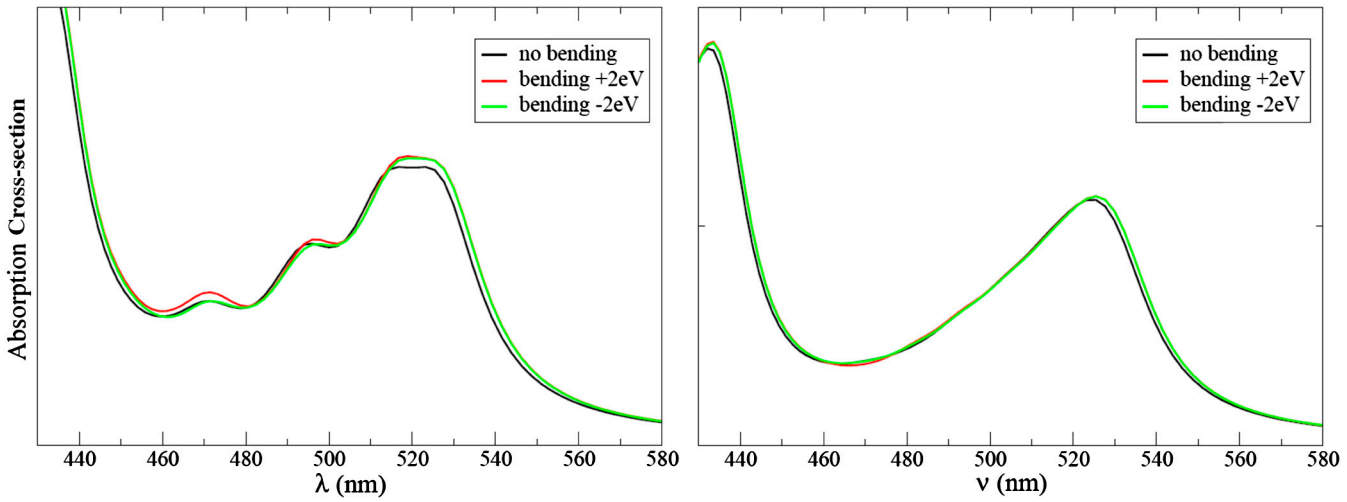

Fig. S5. Absorption cross-section of CdSe nanorods with an aspect ratio of $\xi = 4$ (*Left*) and $\xi = 8$ (*Right*).

Table S1. The quasiparticle gaps

ξ	CdSe (eV)	CdS (eV)
1	2.44	3.27
2	2.30	3.13
3	2.28	3.11
4	2.27	3.10
5	2.26	3.10
6	2.26	3.10
7	2.26	3.09
8	2.26	3.09